Molecular Crystals and Liquid Crystals
Publication details, including instructions for authors and subscription information:
http://www.tandfonline.com/loi/gmcl20

Dark Spatial Solitons in Liquid Crystals

Armando Piccardi [a] , Alessandro Alberucci [a] & Gaetano Assanto [a]
[a] NooEL, NonLinear Optics and OptoElectronics Lab, University "ROMA TRE", Via della Vasca Navale 84, Rome, Italy
Version of record first published: 18 Apr 2012.

To cite this article: Armando Piccardi , Alessandro Alberucci & Gaetano Assanto (2012): Dark Spatial Solitons in Liquid Crystals, Molecular Crystals and Liquid Crystals, 558:1, 168-175

To link to this article: http://dx.doi.org/10.1080/15421406.2011.654185

Mol. Cryst. Liq. Cryst., Vol. 558: pp. 168–175, 2012

ISSN: 1542-1406 print/1563-5287 online
DOI: 10.1080/15421406.2011.654185

Taylor & Francis
Taylor & Francis Group

Dark Spatial Solitons in Liquid Crystals

ARMANDO PICCARDI,* ALESSANDRO ALBERUCCI, AND GAETANO ASSANTO

NooEL, NonLinear Optics and OptoElectronics Lab, University "ROMA TRE", Via della Vasca Navale 84, Rome Italy

We demonstrate the generation and propagation of dark spatial solitons in dye-doped nematic liquid crystals, exploiting a defocusing nonlinearity stemming from a reduced order parameter. Good agreement is obtained between the experimental measurements and a simplified model. Moreover, a probe beam is used to confirm the guiding properties of the soliton.

Keywords Dark solitons; dye-doped nematic liquid crystals; order parameter

1. Introduction

Interactions between nematic liquid crystals (NLC) and electric fields, both at low and optical frequencies, have been extensively investigated in the last decades [1–4]. In optics, such kinds of dipolar interactions usually result in the change of the refractive index felt by an incoming beam, thus being sources of different kinds of nonlinearities [5]. In fact, when sandwiched between two interfaces and provided with alignment to ensure long range bulk order, NLC are equivalent to a positive uniaxial crystal, with optic axis directed as the long axis of the elongated molecules, namely the molecular director $\boldsymbol{n}$. In this case, the ordinary refractive index (n_o) corresponds to the index $n_\perp$ perpendicular to the director, while the extraordinary index is $n_e = n_e\,(\theta)$, with θ the angle between the director and the electric field and $n_e\,(0) = n_\parallel$, being $n_\parallel$ the index associated to the direction along the director [6]. At relatively low intensities, the induced dipoles result in an optical torque which tends to align the director towards the field; thus, the reorientational effect is dominant and the beam undergoes self-focusing. When the latter balances linear diffraction, a spatial soliton is formed [7,8].

Optical spatial solitons have been widely studied in a variety of materials [9–18], including their fundamental properties and their character of self-induced waveguides which makes them suitable for novel generations of signal routers. The most common "*bright*" spatial solitons are bell-shaped beams stemming from a self-focusing nonlinearity [19,20]; NLC are known to support stable (2D + 1)D bright spatial solitons or "*nematicons*", relying on both the reorientational nonlinearity [21] and their inherent nonlocality [22,23]. Self-localization via the thermo-optic response was also investigated [24,25]. Conversely, "*dark*" spatial solitons are intensity notches in a uniformly bright background, with a π phase jump

*Address correspondence to Armando Piccardi, NooEL, NonLinear Optics and OptoElectronics Lab, University "ROMA TRE", Via della Vasca Navale 84, Rome Italy. E-mail: apiccardi@uniroma3.it

on axis; they can exist in self-defocusing materials [26]. Dark or "gray" (i.e., beams with a phase jump different from π) self-confined structures have been experimentally investigated in realistic settings with finite background in various materials [27–30], demonstrating their character of self-induced waveguides in analogy with bright solitons [31]; in fact, a positive graded index profile results in the intensity dip due to light induced refractive index decrease in the surrounding illuminated regions [26].

In this paper we present the first experimental observations of "*dark nematicons*", i.e. dark spatial solitons in nematic liquid crystals (NLC) with a self-defocusing response. Rather than exploiting a thermal (defocusing) nonlinearity, we employed a small amount of dye doping. This is known to modify the NLC response introducing resonant absorption and one or more of: reorientation enhancement [32,33], reduction [34], nonlinearity inversion [35] and surface effects [36,37], depending on the particular guest dye and its interaction with the NLC host. We used a dye able to modify the NLC molecular order parameter (S) [6] upon (resonant) illumination.

2. Sample Characterization

We used a mixture of the commercial 5CB ($n_{\|} \approx 1.7$, $n_{\perp} \approx 1.5$ in the visible) with the mesogenic azo-dye CPND [38] (10% in weight), sandwiched between two parallel glass interfaces separated by $9\,\mu m$. The inner surfaces were treated in order to obtain homeotropic anchoring of the NLC molecules, providing a director perpendicular to the interfaces, as sketched in Fig. 1.

The interaction between the mixture and light of wavelength within its absorption band is known to generate a rearrangement of the NLC molecules around the dye molecules in the excited state: the net effect is a lowering of the order parameter [39]. The latter, defined as $S = 1/2 \int d\xi f(\xi)(3\cos^2\xi - 1)$, is a scalar quantity describing the second order momentum of the molecular distribution, with ξ the angle between the director and the symmetry axis of the single molecule and $f(\xi)$ the molecular distribution. $S = 0$ corresponds to the fully disordered (isotropic) state, while $S = 1$ indicates that all the molecules are aligned along the same direction; at room temperatures, the nematic phase has values of S typically around 0.6–0.7. Rather than the microscopic analysis of the material, we are interested in its link to macroscopic optical properties, such as absorption and the refractive indices: the extraordinary (ordinary) refractive index tends to increase (decrease) linearly with the order parameter, with a material dependent coefficient [39].

To verify the self-defocusing character of the mixture, we launched a $\lambda = 532nm$ beam in the sample with a waist of about 2 μm, monitoring by a CCD camera the light scattered out of the propagation plane. Owing to the dye, the beam generates a non-uniform distribution of the order parameter and thus of the refractive indices; Fig. 1 shows some of the acquired images of beam evolution. At low power, i.e. in the linear regime, the

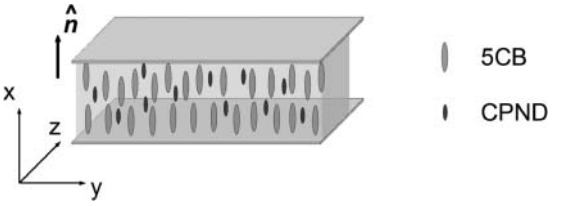

Figure 1. Sample sketch. The homeotropically aligned mixture is the NLC 5CB with 10% in weight of the dye CPND.

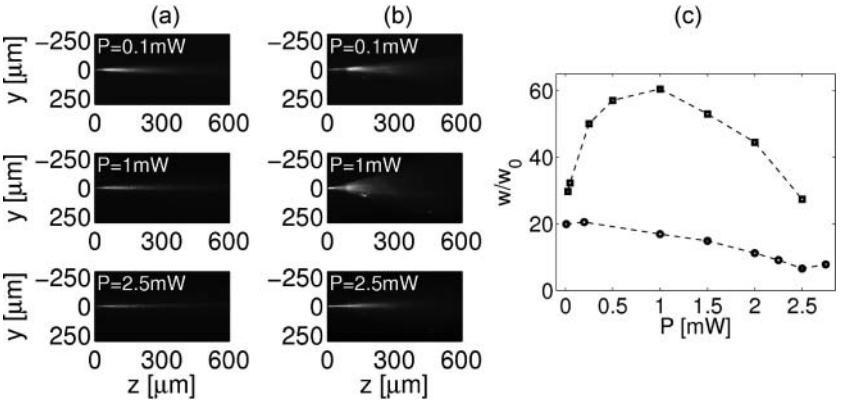

Figure 2. Material characterization. The change in order parameter has a focusing effect on the (a) ordinary polarization, and a defocusing effect on the (b) extraordinary polarization. (c) Normalized waist (w_0 is the value in $z = 0$) versus input power for o- (circles) and e- (squares) beams. The non-monotonic behavior of the latter is due to saturation of the nonlinearity.

beam diffracts for both ordinary and extraordinary polarizations, with its transverse profile widening consistently with the anisotropy of NLC. At higher powers, the reduction of the order parameter results in a net increase of the ordinary refractive index (electric field parallel to *y*): the beam undergoes self-focusing, as it can be seen by the decrease in waist versus power (Fig. 2(a,c)). On the other hand, the extraordinary wave experiences a negative refractive index profile, with a resulting self-defocusing of the beam polarized along *x*: beam spreading becomes larger than in the linear case (Fig. 2(b,c)); the non-monotonic trend of the extraordinary beam can be ascribed to saturation effects due to the finite dye concentration.

To exclude the occurrence of thermal effects in the power regime under investigation, we numerically verified that such variation of refractive indices would be associated to temperatures well beyond the isotropic transition value. Thus, a thermal nonlinearity cannot be responsible for such defocusing, to be attributed to the dye-mediated variation of the order parameter.

3. Model

We can model the electromagnetic propagation by a unidimensional nonlinear Schrödinger equation:

$$2ik_0n_0\frac{\partial A}{\partial z} + D\frac{\partial^2 A}{\partial y^2} + i\alpha A + 2k_0^2 n_0 \Delta n(|A|^2)A = 0 \tag{1}$$

where k_0 is the vacuum wavenumber, n_0 the linear refractive index, A the field envelope, D the diffraction coefficient, α the wavelength dependent absorption coefficient (due to the presence of the dye) and Δn the nonlinear change in refractive index (in our case due to molecular order variations); we choose a saturable expression for Δn:

$$\Delta n = \frac{n_2 I}{1 + I/I_{sat}} \tag{2}$$

with $I = |A|^2$, I_{sat} a saturation intensity and n_2 the effective nonlinear coefficient, its sign being either positive or negative, depending on ordinary or extraordinary beam polarization, i. e., for focusing or defocusing all-optical nonlinearities, respectively.

We numerically solved Eq. (1) considering an extraordinary polarized Gaussian beam, with a π phase jump at the center of its profile: the resulting intensity profile consists of two bright lobes separated by a notch. This choice (rather than a plane wave) was intended to better reproduce the actual experimental conditions described below. Figure 3 shows the calculated beam evolution for various initial powers: in the linear regime the notch and the lobes spread as a whole, as expected from a beam with this phase distribution. As the power increases the bright lobes diffract more due to negative nonlinearity, while the dark notch starts to self-confine, eventually keeping its profile constant versus propagation. At higher powers, as saturation effects become more effective with larger intensities, the bright lobes reduce their spreading, while the notch maintains its self-confined character.

5. Experiments

To observe a dark nematicon, we launched a Gaussian beam with a waist of about 10 μm into the sample using a microscope objective. To introduce the π phase shift we inserted the edge of a thin glass slide in the beam center, tilting it until the different optical paths in the two regions induced a zero intensity dip [30]. Nonlinear beam propagation was studied by evaluating the full width at half maximum (FWHM) of the dark notch from the acquired images, as a function of propagation distance and power.

Typical results are graphed in Fig. 4 for the extraordinary polarization (defocusing nonlinearity): up to P = 1 mW linear diffraction is dominant, the notch as well as the

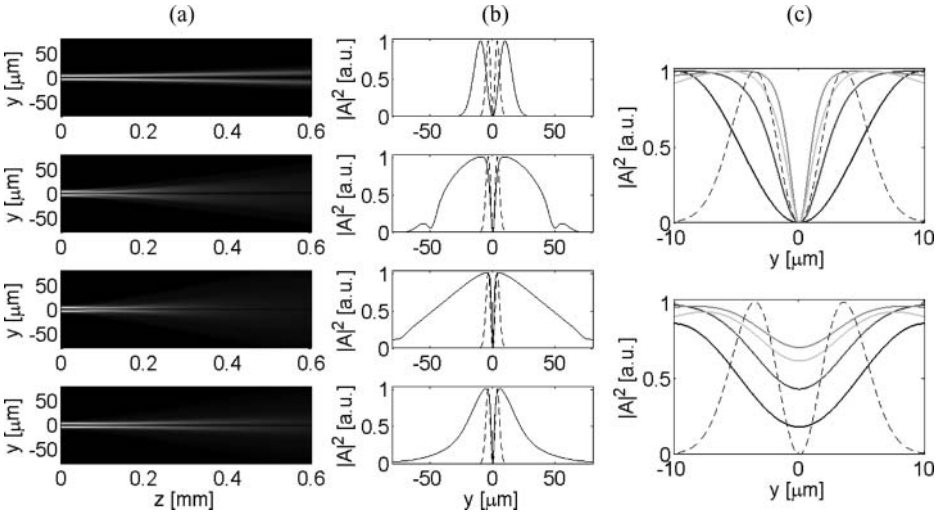

Figure 3. Numerical results for an extraordinarily polarized Gaussian beam with a π phase jump in y = 0. (a) Beam propagation for power densities of 1×10^{-6}, 5×10^{3}, 1×10^{5}, and 5×10^{5} Wm^{-1}, from top to bottom, respectively. (b) Input (dashed lines) and output (solid lines) intensity profiles corresponding to powers as in (a). (c) Detail of the intensity profiles (dashed ines for input profiles), with effects due to nonlinear saturation; powers are the same as in (a), increasing from the darkest to the lightest line. In the bottom panel the blurring is accounted for, with nonzero intensity at the center of the notch.

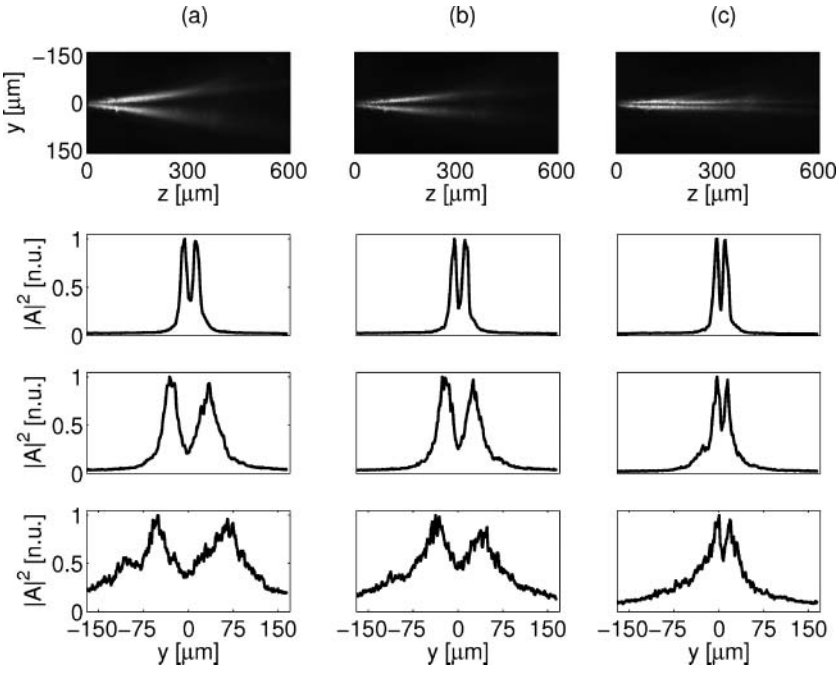

Figure 4. Propagation of a dark soliton in NLC. Acquired images (first row) and intensity profiles in z = 0 (second row), 300 μm (third row), 600 μm (fourth row) for (a) 1, (b) 2, (c) 4 mW input power, respectively. The diffraction at low power is compensated by nonlinear defocusing and the notch self-confines. The bright lobe spreading is limited by saturation effects and losses.

bright humps widen (Fig. 4(a)). Increasing power the notch gradually reduces its width (Fig 4(b)); when $P = 4\ mW$ the FWHM is nearly constant in propagation, as visible in Fig. 4(c), while the lobes do not spread further, reproducing well the numerical predictions. Beyond this power value thermal effects began to be non negligible, preventing the correct evaluation of the beam profile. We stress that the nonzero intensity at the notch is due to the blurring associated to scattering in NLC, as we accounted for in the FWHM calculation (see Fig. 3(c), bottom graph). Figure 5 graphs a synopsis of experimental results versus propagation distance (Fig. 5(a)) and input power (Fig. 5(b)), respectively.

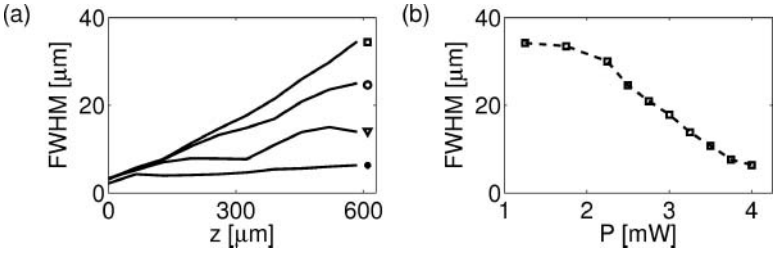

Figure 5. Width of the dark notch. In (a), square, circle, triangle and filled circle correspond to P = 1,2, 3, 4 mW, respectively. (b) The output FWHM (in z = 500 mm) versus power shows an intensity dip becoming narrower and narrower, until it eventually settles to a width as large as the input value.

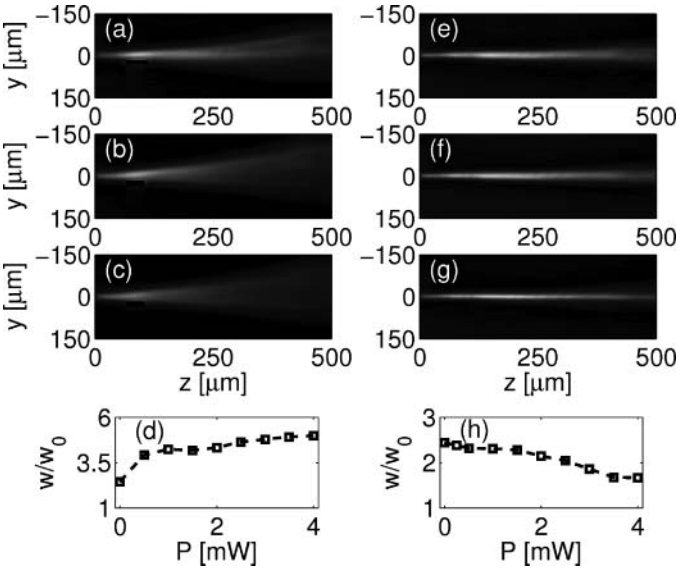

Figure 6. Guiding properties of the dark-nematicon. (a–c) Low power (P = 10 μW) ordinarily polarized probe launched within the notch, for the green input at P = 1, 2, 4 mW, respectively. (d) Normalized waist versus input soliton power. (e–g) Same as in (a) thru (c) but for the extraordinary polarization: as the dark soliton is formed, the refractive index profile guides a collinear co-polarized probe, as apparent from (h) the measured waist versus soliton power.

So far we demonstrated that, for an excitation in the extraordinary polarization, the material exhibits a defocusing nonlinearity, with an intensity dip in the beam self-trapping as the power increases up to 4 mW. To confirm that we are in the presence of a dark spatial soliton, we checked its guiding properties by injecting a weak probe beam.

We launched a beam at a different wavelength (outside the absorption band of the guest-host) collinear with the notch: a Gaussian beam at $\lambda = 1064\ nm$ was focused to a waist of about 5 μm (roughly the width of the dark stripe) and a power low enough to avoid the insurgence of any nonlinear effects ($P = 10\ \mu W$). When ordinarily polarized (Fig. 6(a)), the probe experiences a negative index gradient, with a resulting defocusing: the probe waist increases with power. Conversely, when probe and dark nematicon are copolarized, the former senses a positive index gradient and becomes transversely confined in the dark notch.

6. Conclusions

We reported the observation of dark spatial solitons in dye-doped nematic liquid crystals. The negative nonlinearity was provided by a change in the order parameter, as induced by the interaction between light and a mixture of NLC with an azo-dye. A simplified model accounting for nonlinearity saturation reproduces well the experimental results. The guiding properties of the dark solitons were tested with a collinear low power probe outside the guest-host absorption band.

Acknowledgments

We thank Dr. N. Tabyrian and Beam Engineering for Advanced Measurements Company (USA) for providing the samples. A. A. thanks "Regione Lazio" for a generous grant.

References

[1] Yang, D. K., & Wu, S. T. (2006), *Fundamentals of Liquid Crystals Devices*, Wiley.
[2] Margerum, J., Nimoy, J., & Yong, S. (1970). *Appl. Phys. Lett.*, *17*, 51.
[3] Herman, R. M., & Serinko, R. J. (1979). *Phys. Rev. A*, *19*, 1757–1769.
[4] Durbin, S. D., Arakelian, S. M., & Shen, Y. R. (1981). *Opt. Lett.*, *6*, 411–413.
[5] Khoo, I. C. (2009). *Phys. Rep.*, *471*, 221.
[6] Simoni, F. (1997). *Nonlinear Optical Properties of Liquid Crystals*, World Scientific: Singapore.
[7] Peccianti, M., Conti, C., Assanto, G., De Luca, A., & Umeton, C. (2004). *Nature*, *432*, 733.
[8] Peccianti, M., Assanto, G., De Luca, A., Umeton, C., & Khoo, I. C. (2000). *Appl. Phys. Lett.*, *77*, 7–9.
[9] Bjorkholm, J. E., & Ashkin, A. A. (1974). *Phys. Rev. Lett.*, *32*, 129–132.
[10] Duree, G. C., Shultz, J. L., Salamo, G. J., Segev, M., Yariv, A., Crosignani, B., Di Porto, P., Sharp, E. J., & Neurgaonkar, R. R. (1993). *Phys. Rev. Lett.*, *71*, 533–536.
[11] Torruellas, W. E., Wang, Z., Hagan, D. J., VanStryland, E. W., Stegeman, G. I., Torner, L., & Menyuk, C. R. (1995). *Phys. Rev. Lett.*, *74*, 5036–5039.
[12] Di Falco, A., & Assanto, G. (2003). *IEEE Photon. Technol. Lett.*, *15*, 537–9.
[13] Leo, G., Colace, L., Amoroso, A., Di Falco, A., & Assanto, G. (2003). *Opt. Lett.*, *28*, 1031–1033.
[14] Leo, G., Amoroso, A., Colace, L., Assanto, G., Roussev, R. V., & Fejer, M. M. (2004). *Opt. Lett.*, *29*, 1778–17780.
[15] Pasquazi, A., Stivala, S., Assanto, G., Gonzalo, J., Solis, J., & Afonso, C. (2007). *Opt. Lett.*, *32*, 2103–2105.
[16] Gallo, K., Pasquazi, A., Stivala, S., & Assanto, G. (2008) *Phys. Rev. Lett.*, *100*, 053901.
[17] Conti, C., D'Asaro, E., Stivala, S., Busacca, A. C., & Assanto, G. (2010). *Opt. Lett.*, *35*, 3760–3762.
[18] Rotschild, C., Cohen, O., Manela, O., Segev, M., & Carmon, T. (2005). *Phys. Rev. Lett.*, *95*, 213904.
[19] Kivshar, Y. S., & Agrawal, G. P. (2003). *Optical Solitons*, Academic: San Diego.
[20] Conti, C., & Assanto, G. (2004). *Enc. of Modern Optics. Oxford: Elsevier*, *5*, 43–55.
[21] Assanto, G., & Karpierz, K. (2009). *Liq. Cryst.*, *36*, 1161.
[22] Bang, O., Krolikowski, W., Wyller, J., & Rasmussen, J. J. (2002). *Phys. Rev. E*, *66*, 046619.
[23] Conti, C., Peccianti, M., & Assanto, G. (2004). *Phys. Rev. Lett.*, *92*, 113902.
[24] Derrien, F., Henninot, J. F., Warenghem, M., & Abbate, G. (2000). *J. Opt. A: Pure Appl. Opt.*, *2*, 332.
[25] Warenghem, M., Blach, J. F., & Henninot, J. F. (2008). *J. Opt. Soc. Am. B*, *25*, 1882.
[26] Kivshar, Y. S., & Luther-Davies, B. (1998). *Phys. Rep.*, *298*, 81–197.
[27] Hasegawa, A., & Tappert, F. (1973). *Appl. Phys. Lett.*, *23*, 171.
[28] Allan, G. R., Skinner, S. R., Andersen, D. R., & Smirl, A. L. (1991). *Opt. Lett.*, *16*, 156.
[29] Andersen, D. R., Hooton, D. E., Grover, J., Swartzlander, A., & Kaplan, A. E. (1990). *Opt. Lett.*, *15*, 783.
[30] Duree, G., Morin, M., Salamo, G., Segev, M., Crosignani, B., Di Porto, P., Sharp, E., & Yariv, A. (1995). *Phys. Rev. Lett.*, *74*, 1978.
[31] Luther-Davies, B., & Xiaoping, Y. (1992). *Opt. Lett.*, *17*, 496.
[32] Janossy, I., Lloyd, A., & Wherrett, B. (1990). *Mol. Cryst. Liq. Cryst.*, *179*, 1.
[33] Piccardi, A., Alberucci, A., & Assanto, G. (2010). *Phys. Rev. Lett.*, *104*, 213904.
[34] Janossy, I. (1994). *Phys. Rev. E*, *49*, 2957.
[35] Khoo, I. C., Li, H., & Liang, Y. (1993). *IEEE J. Quantum Electron*, *29*, 1444–1447.

[36] Ouskova, E., Reznikov, Y. S., Shiyanovskii, V., Su, L., West, J. L., Kuksenov, O. V., Francescangeli, O., & Simoni, F. (2001). *Phys. Rev. E*, *64*, 051709.
[37] Piccardi, A., Assanto, G., Lucchetti, L., & Simoni, F. (2008). *Appl. Phys. Lett.*, *93*, 171104.
[38] Mesogenic Azo-Dye CPND supplied by BEAM, http://www.beamco.com
[39] De Gennes, P. G., & Prost, J. (1993). *The Physics of Liquid Crystals*, Oxford Science, New York.